

## Theoretical study of the non-local optical potential in EXAFS spectra

Keisuke Hatada,<sup>a,\*</sup> Takashi Fujikawa<sup>a</sup> and Lars Hedin<sup>b</sup>

<sup>a</sup>Graduate School for Science, Chiba University, Inage, Chiba 263-8522, Japan, and <sup>b</sup>Department of Physics, Lund University, Sölvegatan 14A, S-223 62 Lund, Sweden. E-mail: hatada@scichem.s.chiba-u.ac.jp

We study the optical potential effects on the extended x-ray absorption fine structure (EXAFS) and x-ray photoelectron diffraction (XPD) spectra. For the valence electron optical potential we use a local density approximation because the charge density changes fairly slowly, whereas we use a non-local optical potential for the core electron part based on GW-approximation. In the Br K-edge EXAFS spectra the present optical potential gives rise to the phase difference and the amplitude reduction; the agreement with the experimental result is excellent. In the N-1s XPD spectra for N<sub>2</sub>/Ni(100), the spherical wave effects enhance the effects due to the optical potential.

**Keywords:** optical potential; GW approximation; EXAFS.

### 1. Introduction

Elastic and inelastic scattering of electrons provides useful information on atomic structure and properties of bulk solids as well as solid surfaces.

It has long been recognized that elastic scattering of electrons is determined by the self-energy for the one-electron Green's function (optical potential), and its associated one-electron damping function (Bell & Squires, 1959; Hedin & Lundqvist, 1969), and explicit discussions have been made for XPS (Bardyszewski & Hedin, 1985), EXAFS (Hedin, 1988; Fujikawa, 1999) and EELFS (Fujikawa & Hedin, 1989; Fujikawa, 1991, 1992).

Hedin and Lundqvist (HL) (1971) suggested a scheme based on the Sham and Kohn theory (1971), where the electron gas self-energy  $\Sigma_0(q, \varepsilon(q))$  is used with a density dependent momentum  $q(\mathbf{r})$ . Following Hedin and Lundqvist (1971) several authors applied such a local density potential to electron scattering from atoms in the intermediate energy region, using the plasmon pole approximation to the GW self-energy, and showed that this potential gives an excellent description of the EXAFS calculation (Lee & Beni, 1977; Mustre de Leon *et al.*, 1991). In general the Hedin-Lundqvist potential gives good results, however, the results are not so clear-cut; sometimes we can find a value  $\alpha$  in  $X_\alpha$  potential which gives a better result than the Hedin-Lundqvist potential (Woolfson *et al.*, 1982).

We have earlier developed a theory for a practical, self-consistent and non-local optical atomic potential in a solid (Fujikawa *et al.*, 1993, 2000) and applied it to electron scatterings from He (Fujikawa *et al.*, 1995a), Ne, Ar and Kr (Fujikawa *et al.*, 1998), atoms in metals, semiconductors and insulators (Fujikawa *et al.*, 2000), where good agreement with the experimental results was obtained.

In this work we apply our optical potential theory to EXAFS and XPD analyses to study the importance of dynamic polarization effects on these spectra.

### 2. Theory

Detailed discussions of the crystal potential have been given long ago by Hedin (1965a, 1965b; Hedin & Lundqvist, 1969). In Hedin and Lundqvist (1969), p. 129, the following expression for the self-energy (optical potential) is given,

$$\begin{aligned} \Sigma_0 &= G^c W + G^v W^v P^c W^v + G^v W^v + \dots \\ &\cong V_{ex}^c + V_{pol}^c + \Sigma^v. \end{aligned} \quad (1)$$

Here  $G^v W^v$  is the self-energy from the valence electrons  $\Sigma^v$ , while  $G^c W$  is the core exchange  $V_{ex}^c$  and  $G^v W^v P^c W^v$  the screened polarization potential from the ion cores  $V_{pol}^c$ . The second term is simplified after we introduce some approximations (Fujikawa *et al.*, 1993, 2000),

$$V_{pol}^c(x, x'; \omega) = A(\mathbf{r}, \mathbf{r}') G(x, x'; \omega - \Delta), \quad (2)$$

where  $A(\mathbf{r}, \mathbf{r}')$  is the polarization term which does not depend on energy and  $G(x, x'; \omega - \Delta)$  is the scattering Green's function shifted by the averaged excitation energy  $\Delta$ . This optical potential is non-local and can be solved self-consistently.

### 3. Results and discussion

#### 3.1. Application to Br K-edge EXAFS spectra

As an example we apply our non-local optical potential theory to the analyses of K-edge EXAFS spectra of the Br<sub>2</sub> molecule. The K-edge EXAFS oscillation is given, in the single scattering curved wave approximation (Fujikawa *et al.*, 1995b)

$$\chi(k) = \chi^p(k) + \chi^s(k), \quad (3)$$

$$\begin{aligned} \chi^p(k) &= \sum_{\alpha} \frac{1}{k(R_{\alpha}^0)^2} \text{Im} \left[ \exp\{2i(kR_{\alpha}^0 + \delta_1^A)\} \tilde{f}_{\alpha}(\pi; R_{\alpha}^0) \right. \\ &\quad \times \exp \left\{ \sum_{n=1} (2ik)^n \langle \Delta_{\alpha}^n \rangle_c \right\} \Big], \end{aligned} \quad (4)$$

$$\begin{aligned} \chi^s(k) &= \sum_{\alpha} \frac{1}{k(R_{\alpha}^0)^2} \text{Im} \left[ \exp\{2i(kR_{\alpha}^0 + \delta_1^A)\} \tilde{f}_{\alpha}^1(\pi; R_{\alpha}^0, T) \right. \\ &\quad \times \exp(-2k^2 \langle \Delta_{\alpha}^2 \rangle_c) \Big], \end{aligned} \quad (5)$$

which has temperature dependent dynamical spherical wave part  $\chi^s$  in addition to dynamical plane wave part  $\chi^p$ . Here  $R_{\alpha}^0$  is the equilibrium distance between  $\alpha$  and A atoms (A is the X-ray absorbing atom) and  $\Delta_{\alpha}$  is relative displacement of the pair,  $\tilde{f}_{\alpha}(\pi; R_{\alpha}^0)$  and  $\tilde{f}_{\alpha}^1(\pi; R_{\alpha}^0, T)$  are the static and the dynamic back scattering spherical wave amplitudes; the latter depends on temperature. As input data for the calculation, we use  $R_{\alpha}^0 = 2.2836\text{\AA}$ , cumulants  $\langle \Delta_{\alpha} \rangle_c = 0.00431\text{\AA}$  and  $\langle \Delta_{\alpha}^2 \rangle_c = 0.00199\text{\AA}^2$  respectively. These parameters are deduced from previous experimental data (Frenkel & Rehr, 1993; Yokoyama *et al.*, 1996).

Figure 1 compares the calculated K-edge EXAFS spectra of Br<sub>2</sub> molecule by use of the Hartree-Fock (HF), Hartree-Fock for core electrons and Hedin-Lundqvist for valence electrons (HF+HL) and the present optical potential (FH). Referring to Eq. (1) the HF potential uses the non-local exchange potential for total electrons, the HF+HL potential uses both the third term  $\Sigma^v$  and the first term  $V_{ex}^c$ , and the FH potential has in addition the non-local polarization potential  $V_{pol}^c$ . The calculated result shows that the optical potential

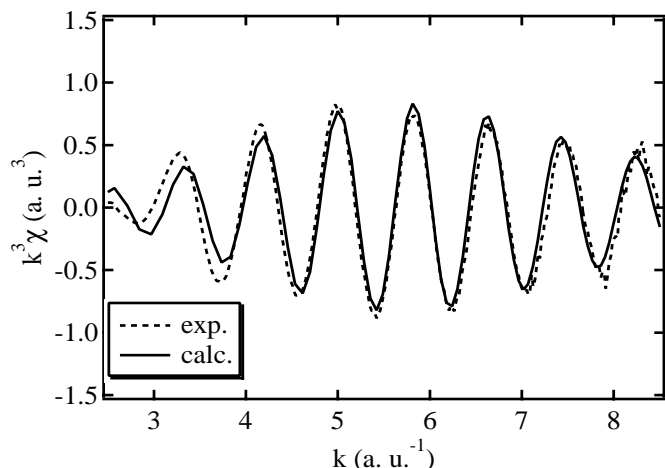


**Figure 1**  
Calculated EXAFS spectra of Br<sub>2</sub> for HF (dotted line), HF+HL (dashed line) and FH (solid line) potentials.

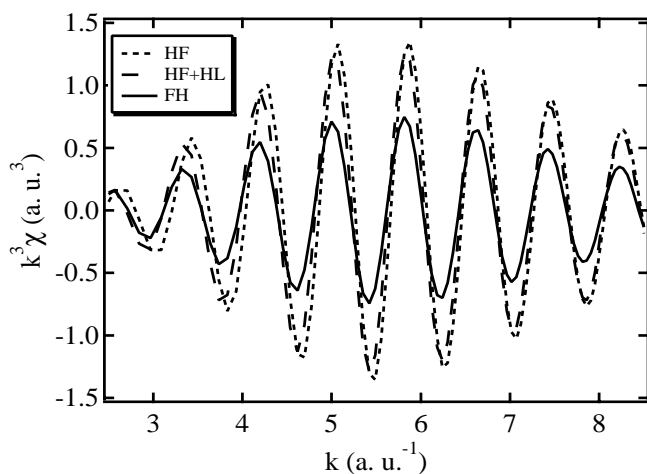


**Figure 2**  
Comparison of theoretical (solid line) and experimental (dotted line) EXAFS spectra of Br<sub>2</sub> (Filipponi & D'Angero, 1998). For the theoretical calculation we use the FH optical potential.

is responsible for the EXAFS amplitude reduction and the phase shift as demonstrated by Lee and Beni (1977). The FH potential gives rise to a pronounced reduction whereas only a small phase difference compared to the HL potential.

Figure 2 shows the comparison of the theoretical (solid line) and the experimental (dotted line) EXAFS spectrum of Br<sub>2</sub> molecule. The theoretical spectrum calculated by using the FH optical potential is compared with the experimental one measured by Filipponi and D'Angero (1998). The calculated result is excellent; our optical potential is promising for the EXAFS analyses.

### 3.2. Application to N-1s XPD spectra for N<sub>2</sub>/Ni(100)

Back scattering of photoelectrons plays a central role in EXAFS analyses, while in XPD analyses forward scattering play an important role because of strong anisotropy in the scattering amplitude; we observe sharp peak in the scattering intensity. So far we have

investigated many-body effects on the angular distribution of elastically scattered electrons from atoms in solids, and we found the large influence on small-angle scattering amplitude (Fujikawa *et al.*, 2000). Therefore it is interesting to apply our optical potential theory to XPD calculations.

The XPD intensity for measuring photoelectron momentum **k** is written in the spherical wave formula (Fujikawa *et al.*, 1995b)

$$\begin{aligned}
 I(\mathbf{k})_c &\propto |Z_1 + Z_2 + Z_3 + \dots|^2 \\
 &= |Z_1|^2 + 2\text{Re}(Z_1^* Z_2) + |Z_2|^2 + \dots \\
 &= A + B + C + \dots,
 \end{aligned}
 \tag{6}$$

where Z<sub>1</sub> (direct term) and Z<sub>2</sub> (single scattering term) are explicitly shown

$$Z_1 = \sum_L Y_L(\hat{\mathbf{k}}) M_{LL_c}, \tag{7}$$

$$\begin{aligned}
 Z_2 &= \sum_{\alpha \neq A} \exp(-i\mathbf{k} \cdot \mathbf{R}_\alpha) \\
 &\times \sum_{L'} \sum_L Y_{L'}(\hat{\mathbf{k}}) t_{l'}^\alpha(k) G_{L'L}(k\mathbf{R}_\alpha) (-1)^{l+l'} M_{LL_c}.
 \end{aligned}
 \tag{8}$$

Here M<sub>LL<sub>c</sub></sub> is the atomic photoexcitation matrix element from a core with angular momentum L<sub>c</sub> and G<sub>L'L</sub> is the angular momentum representation of the free propagator, **R**<sub>α</sub> is a position from an emitter atom to a scattering atom α. We calculate the N-1s XPD spectra of N<sub>2</sub> on Ni(100) measured Nilsson *et al.* (1991). The N<sub>2</sub> molecules are chemisorbed perpendicularly to the Ni surface, and we can distinguish the inner from the outer nitrogen using chemical shift. In

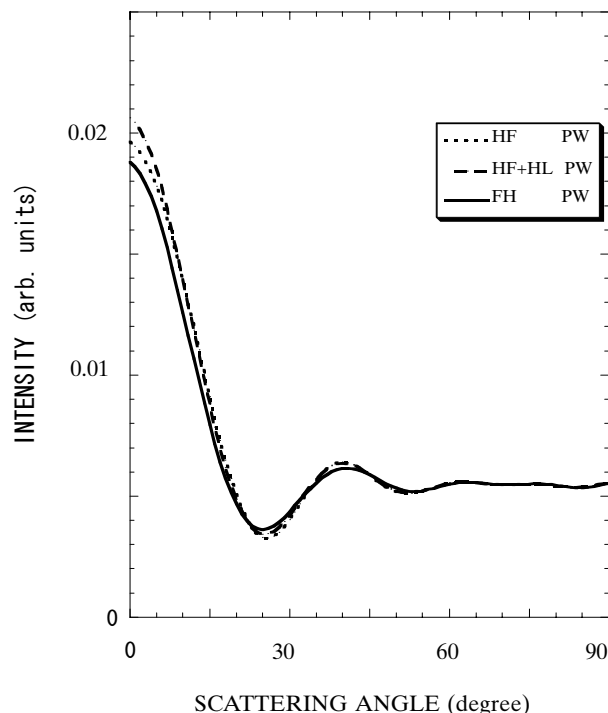


**Figure 3**  
The calculated N 1s XPD spectra from N<sub>2</sub>/Ni(100) show the comparison for the three different potentials HF, HF+HL and FH potentials. Kinetic energy of photoelectrons is 1085.9 eV (Al K<sub>α</sub> excitation). Plane wave approximation is used.

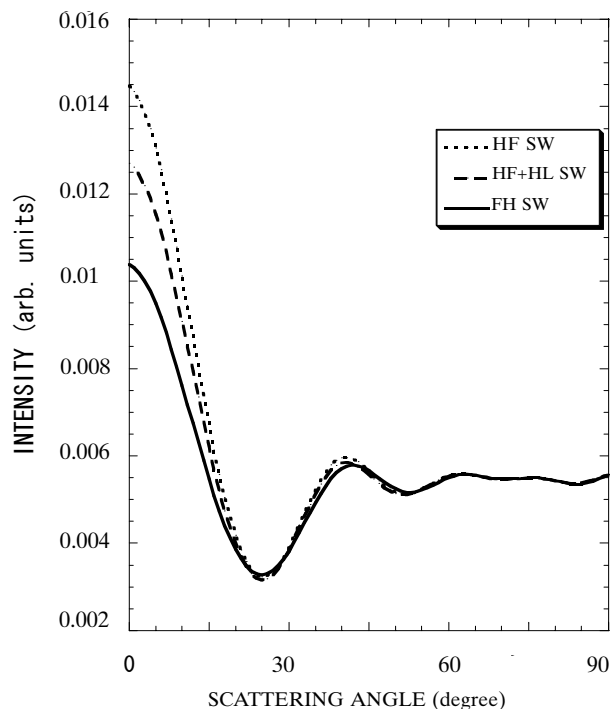


**Figure 4**

The same as in Fig. 3, but for the spherical wave calculations.

this calculation we neglect Debye-Waller factor and the scatterings by Ni substrate atoms for simplicity. Of course they are important for the XPS intensity in large  $\theta$  region. We consider the XPD spectra from the inner atom where the forward scatterings play an important role in the normal emission ( $\theta \approx 0^\circ$ ). Figure 3 compares the calculated XPD spectra for different potentials, where the kinetic energy of photoelectron is 1085.9 eV (Al  $K_\alpha$  excitation) and the plane wave approximation is used. We see that all these models give nearly the same XPD intensity.

Figure 4 shows the same cases as in Fig. 3, but with the spherical wave corrections. The different potentials give rise to larger differences in the SW than in the PW case. In small angle region, the intensity of the interference term  $B = 2\text{Re}(Z_1^* Z_2)$  is ordered as  $B(HF + HL) \sim B(HF) > B(FH)$ , whereas that of  $C = |Z_2|^2$  as  $C(FH) \sim C(HF + HL) > C(HF)$ . Thus the total intensity decreases as,  $I(HF + HL) > I(HF) > I(FH)$  in the PW approximation. Despite that the difference for each term is fairly large, the dif-

ference for the total intensity  $I(\mathbf{k})_c$  is small. On the other hand the intensities of  $B$  and  $C$  are ordered as  $(HF) > (HF + HL) > (FH)$ .

For the SW calculation, the optical potential gives a large phase difference in the interference term, and we observe pronounced differences in XPD intensities for the different potentials.

#### 4. Conclusion

Here, we have applied our non-local optical potential theory to EXAFS and XPD calculations. In EXAFS calculations, the optical potential gives satisfactory results, and is successful to describe the damping effect and the phase difference. In PW XPD calculation, the optical potential has small influence on XPD intensity, though it has large effect on the scattering amplitude. In contrast the optical potential has large influence on the phase factor of the amplitude  $Z_2$  in the SW XPD calculation. Of course the computing time is quite large (300 sec for one SCF calculation) on Pentium III 800 MHz PC.

#### Acknowledgements

The authors are grateful to H. Tanaka and Y. Wada for their help in programming and useful discussion to H. Arai.

#### References

- Bardyszewski, W. & Hedin, L. (1985). *Phys. Scr.* **32**, 439–450.  
 Bell, J. S. & Squires, E. J. (1959). *Phys. Rev. Lett.* **3**, 96–99.  
 Byron, F. W. & Joachain, J. C. (1974). *Phys. Rev. A* **9**, 2559–2568; (1977a). *Phys. Rev. A* **15**, 128–146; (1977b). *J. Phys.* **B10**, 207–226.  
 Filipponi, A. & D'Angero, P. (1998). *J. Chem. Phys.* **109**, 5356–5362.  
 Frenkel, A. I. & Rehr, J. J. (1993). *Phys. Rev. B* **48**, 585–588.  
 Fujikawa, T. (1991). *J. Phys. Soc. Jpn.* **60**, 3904–3919.; (1992). *Surf. Sci.* **269/270**, 55–60.  
 Fujikawa, T., Hatada, K. & Hedin, L. (2000). *Phys. Rev. B* **62**, 5387–5398.  
 Fujikawa, T., Hatada, K., Yikegaki, T. & Hedin, L. (1998). *J. Elect. Spect.* **88-91**, 649–655.  
 Fujikawa, T. & Hedin, L. (1989). *Phys. Rev. B* **40**, 11507–11518.  
 Fujikawa, T., Saito, A. & Hedin, L. (1993). *Jpn. J. Appl. Phys.* **32S-2**, 18–22.  
 Fujikawa, T., Yimagawa, M. & Miyanaga, T. (1995b). *J. Phys. Soc. Jpn.* **64**, 2047–2068.  
 Fujikawa, T., Yikegaki, T. & Hedin, L. (1995a). *J. Phys. Soc. Jpn.* **64**, 2351–2355.  
 Hedin, L. (1965a). *Phys. Rev.* **139**, A796–A823; (1965b). *Arkiv Fysik* **30**, 231–258; (1988). *Physica B* **158**, 344–346.  
 Hedin, L. & Lundqvist, B. I. (1971). *J. Phys. C* **4**, 2064–2083.  
 Hedin, L. & Lundqvist, S. (1969). *Solid State Physics*, edited by F. Seitz, D. Turnbull and H. Ehrenreich, Vol. **23**, 1. New York: Academic Press.  
 Lee, P. A. & Beni, G. (1977). *Phys. Rev.* **B15**, 2862–2883.  
 Mustre de Leon, J., Rehr, J. J., Zabinsky, S. I. & Albers, R. C. (1991). *Phys. Rev. B* **44**, 4146–4156.  
 Nilsson, A., Tillborg, H. & Mårtensson, N. (1991). *Phys. Rev. Lett.* **67**, 1015–1018.  
 Yokoyama, T., Kobayashi, K., Ohta, T. & Ugawa, A. (1996). *Phys. Rev. B* **53**, 6111–6122.